

Synthesis and Crystal Structure of the Trigonal Silver(I) Dithioaurate(I), Ag_3AuS_2

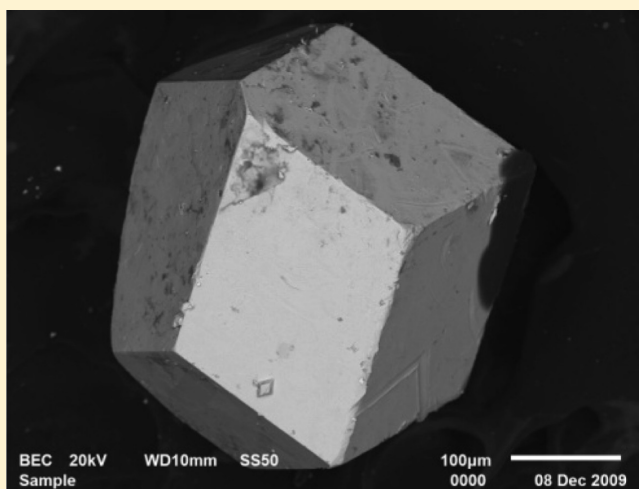
Yu. V. Seryotkin,^{†,‡} V. V. Bakakin,[§] G. A. Pal'yanova,[†] and K. A. Kokh^{*,†}

[†]Institute of Geology and Mineralogy, Russian Academy of Sciences, 3, Koptyuga, 630090 Novosibirsk, Russia

[‡]Novosibirsk State University, 2, Pirogova, 630090 Novosibirsk, Russia

[§]Institute of Inorganic Chemistry, Russian Academy of Sciences, 3, Lavrentieva, 630090 Novosibirsk, Russia

ABSTRACT: Crystals of the silver(I) dithioaurate(I), Ag_3AuS_2 , were obtained by fusing the elements in the required stoichiometric amounts. Single-crystal X-ray analysis showed that two phases of a slightly different composition coexist in the products of synthesis: a trigonal phase [$a = 13.7104(4)$ Å, $c = 17.1170(6)$ Å, space group $R\bar{3}c$] and a cubic one [$a = 19.3590(7)$ Å]. The crystal structure was determined for the first phase. The sublattice of sulfur atoms represents a distorted body-centered cubic packing. The structure contains distinct triatomic linear groups (S–Au–S) and Ag atoms surrounded by four S atoms (from four different linear groups). Comparison was made for the trigonal phase under consideration, cubic petzite (Ag_3AuTe_2) and fischerite (Ag_3AuSe_2) and the tetragonal uytenbogaardtite (Ag_3AuS_2). The trigonal phase Ag_3AuS_2 cannot be attributed to the petzite group, because it is a new structure type. Unlike generally accepted opinion, the tetragonal uytenbogaardtite is not a petzite type either.



INTRODUCTION

Crystals of the silver(I) dithioaurate(I), Ag_3AuS_2 , which is also known as the mineral uytenbogaardtite, with several modifications are described. A single-crystal X-ray structure investigation¹ showed that this compound is cubic with an a of 9.72 Å in space group $P4_32$. The compound synthesized by Graf² according to powder diffraction corresponds to the tetragonal metrics of the unit cell ($a = 9.75$ Å, and $c = 9.78$ Å). The mineral uytenbogaardtite, Ag_3AuS_2 , discovered by Barton et al.³ is also described as a tetragonal one ($a = 9.68$ – 9.76 Å, and $c = 9.78$ – 9.81 Å). Chen et al.⁴ and Wei⁵ found one more low-temperature polymorphic tetragonal modification, Ag_3AuS_2 , liujinyinite ($a = 10.01$ Å, and $c = 11.11$ Å). According to Nekrasov et al.,⁶ phase Ag_3AuS_2 synthesized from elementary Ag, Au, and S at 750 °C and annealed at 300 °C is characterized by the cubic metrics of the unit cell ($a = 9.737$ Å). The X-ray diffraction pattern displays extra lines compared to the tetragonal modification of uytenbogaardtite. In ref 7, the X-ray pattern for uytenbogaardtite synthesized under hydrothermal conditions at 300 °C was comparable to the most typical lines of the tetragonal phase β - Ag_3AuS_2 obtained in ref 2. The X-ray pattern of uytenbogaardtite from the Yunoe deposit matches that of natural uytenbogaardtite³ but lacks the line at 2.124(8) Å.⁸

A variety of results of X-ray diffraction studies with synthetic and natural samples similar in composition demonstrate, at least, a lack of structural information for given compounds. The aim of

this investigation is the synthesis and a study of structural features of silver–gold sulfide of the Ag_3AuS_2 composition.

SYNTHESIS

Crystals of the silver(I) dithioaurate(I), Ag_3AuS_2 , were obtained by fusing the elements in the required stoichiometric amounts. Gold and silver (99.99%) were used as initial materials, in addition to sulfur (99.9%), in amounts of 277.0, 168.4, and 55.0 mg, respectively. Accuracy of weighing is ± 0.05 mg (a Mettler Instrument Ag CH-8606 balance). The synthesis was conducted in evacuated quartz ampules. To avoid losses of volatile sulfur, a quartz rod was put above the charge to occupy the maximal amount of the ampule free volume. The ampules were heated for 3 days at a rate of 0.2–0.5 °C/min to 1050 °C and kept at this temperature for 12 h, and then they were cooled to 700 °C at a rate of 0.2 °C/min and annealed for 3 days. After the annealing had ended, the furnace was switched off and the ampules were cooled to room temperature for ~ 7 h. The experimental solid-phase products were studied by optical and electronic microscopy as well as by X-ray diffraction. The chemical composition of the phases was determined by a Camebax-Micro microanalyzer and LEO-1430VP and JSM-6510LV electron

Received: September 17, 2010

Revised: January 11, 2011

Published: March 07, 2011

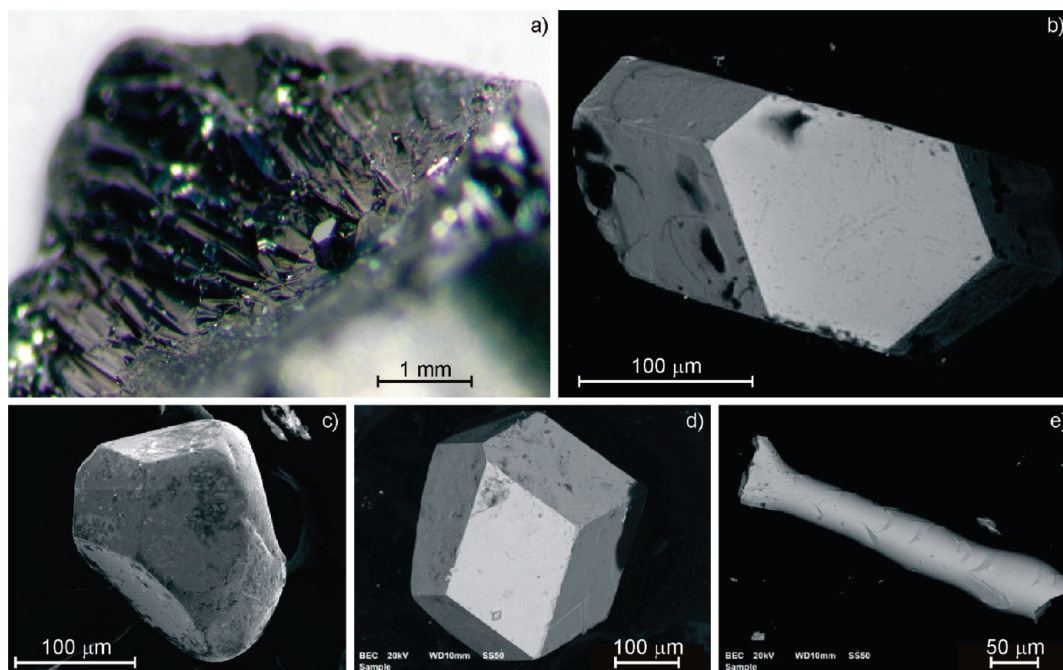


Figure 1. Fragment of the upper part of the synthesized sample (a) and morphology of crystals (b–e, photographed in reflected electrons).

scanning microscopes (JEOL Ltd.) with an INCA Energy 350+ energy-dispersion spectrometer (Oxford Instruments Analytical).

According to the microprobe analysis, the composition of the synthesized compound can be represented as $\text{Ag}_{3.1}\text{Au}_{0.9}\text{S}_2$, the difference between analyses in different points being within the accuracy limit of the method. The synthesized samples are shown in Figure 1a, and the largest crystals are shown in Figure 1b–e. The natural uytenbogaardite crystals found in the Au–Ag epithermal Yunoe deposit (Magadan region, Russia) are similar in appearance.⁹

■ SINGLE-CRYSTAL X-RAY DIFFRACTION STUDY

Well-cut crystals (Figure 1b,c) were selected for a single-crystal experiment. Intensity data were collected with an Oxford Diffraction Gemini R Ultra diffractometer equipped with a CCD, using a graphite monochromator for Mo $K\alpha$ radiation, operated at 50 kV and 30 mA. Data reduction, including a background correction and Lorentz and polarization corrections, was performed with CrysAlis. A semiempirical absorption correction was applied using the multiscan technique.

Two well-cut crystals similar in appearance gave principally different crystallographic characteristics. Their compositions estimated with a scanning electron microscope (LEO1430VP), equipped with an energy spectrometer (Oxford), also vary, $\text{Ag}_{3.29}\text{Au}_{0.71}\text{S}_2$ and $\text{Ag}_{3.05}\text{Au}_{0.95}\text{S}_2$. The metrics of the first (Figure 1c) is cubic with a doubled a parameter [19.3590(7) Å] compared to the literature data.^{1,6} The structure has not yet been determined; this work was devoted to the second crystal (Figure 1b). The metrics of its unit cell is rhombohedrally distorted and pseudocubic [$a = 9.9577(2)$ Å, and $\alpha = 89.263(3)^\circ$]. In deciding on a space group, we preferred $R\bar{3}c$. Solution and refinement of the structure were performed with a hexagonal system. The full experimental details of the data collection and structure determination are listed in Table 1.

The positions of the Au and Ag atoms were determined with direct methods via SHELXS-97,¹⁰ and the S atoms were located

Table 1. Crystallographic and Experimental Data for the Trigonal Phase of $\text{Ag}_{2.94}\text{Au}_{1.06}\text{S}_2$

a (Å)	13.7104(4)
c (Å)	17.1170(6)
V (Å ³)	2786.50(15)
Z	24
space group	$R\bar{3}c$
crystal size (mm)	$0.24 \times 0.12 \times 0.11$
d (g/cm ³)	8.439
diffractometer	Oxford Diffraction Gemini R Ultra
radiation	Mo $K\alpha = 0.71069$ Å
scan type	ω
scan width (deg/frame)	1
exposure (s/frame)	60
2θ range (deg)	8.36–63.48
$h_{\min}, h_{\max}; k_{\min}, k_{\max}; l_{\min}, l_{\max}$	–19, 20; –20, 19; –24, 25
$F(000)$	6094
μ (Mo $K\alpha$) (mm ^{–1})	46.293
no. of I_{hkl} reflections measured	17394
no. of unique F_{hkl}^2	1051
R_{int}	0.0724
no. of observed reflections [$I > 2\sigma(I)$]	930
no. of variables	44
R factors for observed reflections [$I > 2\sigma(I)$]	$R1 = 0.0408$, $wR2 = 0.0749$
R factors for all data	$R1 = 0.0504$, $wR2 = 0.0776$
residual electron density (e/Å ³)	3.359, –3.138

from analysis of difference electron density maps during structure refinement using SHELXL-97.¹¹ During structure refinement in an isotropic approximation, the peak with a maximum at 15 e/Å^3 was revealed near position Ag2 on the difference electron density

Table 2. Atomic Coordinates, Equivalent Isotropic Displacement Parameters $\{U_{\text{eq}} = 1/3 \sum_i [\sum_j (U_{ij} a_i^* a_j^* a_{ij} a_j)]\}$ (square angstroms), and Occupancies for the Trigonal Phase of $\text{Ag}_{2.94}\text{Au}_{1.06}\text{S}_2$

atom	multiplicity, site symmetry	occupancy	x	y	z	U_{eq}
Au1	6 <i>a</i> 32	1	0	0	0.25	0.0168(2)
Au2	18 <i>e</i> .2	1	−0.24555(4)	0	0.25	0.01534(14)
Au3	36 <i>f</i> 1	0.040(3)	−0.1332(10)	0.0371(10)	0.4571(8)	0.023(4) ^a
Ag1	36 <i>f</i> 1	1	0.04698(7)	0.21697(7)	0.33758(5)	0.02220(18)
Ag2	36 <i>f</i> 1	0.96	−0.16159(15)	0.04122(10)	0.42568(10)	0.0461(4)
S1	12 <i>c</i> 3.	1	0	0	0.3869(3)	0.0196(8)
S2	36 <i>f</i> 1	1	−0.1537(2)	0.1806(2)	0.30301(14)	0.0166(4)

^a Au3 position refined isotropically.**Table 3.** Atomic Displacement Parameters (angstroms) for the Trigonal Phase of $\text{Ag}_{2.94}\text{Au}_{1.06}\text{S}_2$

atom	U_{11}	U_{22}	U_{33}	U_{12}	U_{13}	U_{23}
Au1	0.0152(3)	0.0152(3)	0.0199(4)	0.00762(13)	0.000	0.000
Au2	0.01582(19)	0.0152(3)	0.0148(2)	0.00761(13)	0.00112(9)	0.00223(18)
Ag1	0.0195(4)	0.0210(4)	0.0259(4)	0.0100(3)	−0.0012(3)	−0.0053(3)
Ag2	0.0695(9)	0.0284(5)	0.0396(7)	0.0240(6)	0.0277(7)	0.0040(5)
S1	0.0201(13)	0.0201(13)	0.0187(18)	0.0101(6)	0.000	0.000
S2	0.0183(11)	0.0160(10)	0.0172(10)	0.0099(9)	−0.0011(9)	−0.0009(8)

Table 4. Interatomic Distances (angstroms) in the Trigonal Phase of $\text{Ag}_{2.94}\text{Au}_{1.06}\text{S}_2$

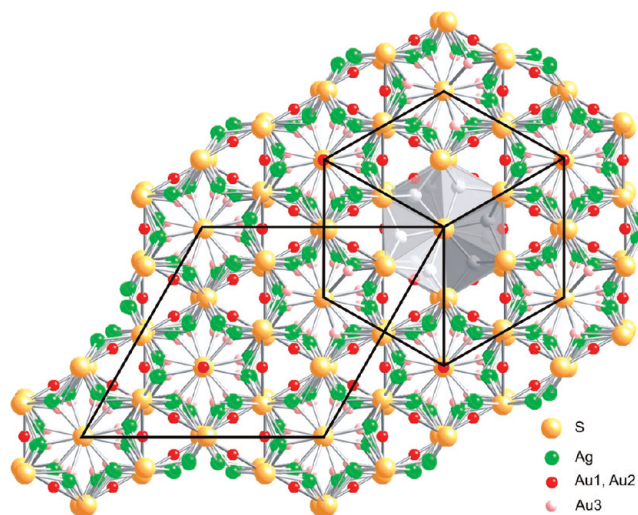
Ag1–S2	2.607(3)	Au2–S2 (two bonds)	2.329(2)
Ag1–S2	2.837(3)		
Ag1–S1	2.8389(16)	Au2–Ag1 (two bonds)	2.9006(9)
Ag1–S2	2.858(3)	Au2–Ag1 (two bonds)	2.9573(8)
		Au2–Ag2 (two bonds)	3.168(2)
Ag2–S2	2.568(3)		
Ag2–S2	2.626(3)	Au3–S1	2.442(12)
Ag2–S1	2.6309(19)	Au3–S2	2.448(12)
Ag2–S2	2.805(3)	Au3–S2	2.678(12)
Ag1–Ag2	3.0062(14)	Au3–Ag2	3.078(13)
Ag1–Ag2	3.0606(15)	Au3–Ag2	3.124(15)
Ag1–Ag1	3.1990(17)	Au3–Ag1	3.206(13)
Ag1–Ag1	3.2405(16)	Au3–Ag1	3.209(12)
Ag2–Ag2	3.115(4)		
		Au3–Ag2 ^a	0.683(13)
Au1–S1 (two bonds)	2.343(4)	Au3–Au3 (two bonds) ^a	2.58(2)
Au1–Ag1 (six bonds)	3.0976(8)		
Au1–Au2 (three bonds)	3.3666(5)		

^a Distances between alternative positions.

map. After structure refinement in an anisotropic approximation, the peak was preserved, though its value decreased to $5.5 \text{ e}/\text{\AA}^3$. The account of this position with 0.06 Au pfu located in it resulted in a decrease in the wR_2 value from 0.0934 to 0.0776. Refined atomic coordinates and displacement parameters are listed in Tables 2 and 3. Interatomic distances and S–Au–S and S–Ag–S angles are listed in Table 4. The structural data are deposited as CIF at the ICSD (CSD No. 422081).

RESULTS AND DISCUSSION

The crystal structure is represented in Figure 2 in projection along the *c* axis. The Ag atoms are located in two

**Figure 2.** Projection of the $\text{Ag}_{2.94}\text{Au}_{1.06}\text{S}_2$ structure along the *c* axis. One of the tube fragments forming the structure by translations of the rhombohedral unit cell is represented with the AgS_4 tetrahedra. The Au3 position, the alternative to Ag_2 , is tinted.

crystallographically inequivalent general positions. There are four S atoms around each silver atom forming an irregular tetrahedron. The Au atoms occupy three crystallographically inequivalent positions, two of which (Au1 and Au2) are fully occupied. Each of them is coordinated by two S atoms at a distance of 2.33–2.34 Å at an S–Au–S angle of 180°; in addition, each Au atom has six Ag atoms as its neighbors at a distance of 2.9–3.2 Å. The third Au position, Au3, is an alternative to position Ag_2 and displaced into the tetrahedron face, gaining a 2+1 coordination by sulfur atoms. According to the structural data, the formula unit can be expressed as $\text{Ag}_{2.94}\text{Au}_{1.06}\text{S}_2$. The difference between the results of the chemical analysis and structural data is mostly caused by errors in the microprobe analysis.

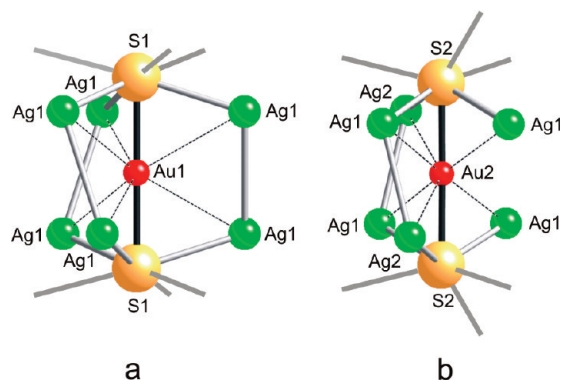


Figure 3. Secondary AuS_2Ag_6 building blocks.

We shall describe the structure in terms of an idealized Ag_3AuS_2 formula without considering the deviation of the composition from a stoichiometry of 1. In doing so, we will emphasize successively both cation components, which in our opinion is useful from a structural and genetic perspective, and anion ones, which is convenient with respect to a comparative and descriptive plan.

The structure contains triatomic linear $\text{S}-\text{Au}-\text{S}$ groups and Ag atoms surrounded by four S atoms (of four different linear groups). The coordination formula (in the formal ionic representation) is $\text{Ag}_3^{[41]}\text{Au}^{[2]}\text{S}_2^{(7)}$, where the coordination number of the cations is enclosed in brackets and that of the anions in parentheses. It is natural that the numbers of cation and anion bonds are equal (the coordination balance rule). Seven bonds of the S^{2-} anion include one bond to Au^+ and six bonds to Ag^+ .

Linear $\text{S}-\text{Au}-\text{S}$ groups, the most rigid fragments, are considered structure-directing elements (templates). It is evident that relatively isometric groups of six Ag^+ atoms from the coordination environment of S^{2-} will be divided each into three-member sets of two types when being pivoted on the $\text{S}-\text{Au}$ bond, i.e., on the template axis. Some of them will remain as if outside the given group, only completing the coordination of its S atoms on the end side. The other ones will be located directly around $\text{S}-\text{Au}$ bonds and will have short $\text{Ag}\cdots\text{Au}$ distances (on the order of ~ 3.0 Å). This results in compact AuS_2Ag_6 groups (Figure 3) along with the initial linear group that has defined the total topology of the configuration at the given coordination formula. The Ag atoms form six-vertex polyhedra around the central Au atom, being intermediate between the trigonal prism and octahedron. The given blocks may be considered as secondary building units (structure blocks) for constructing the whole structure. In the process of construction, the blocks combine a portion of the edges of AuAg_6 polyhedra to form a three-dimensional AuAg_3 net with the sulfur atoms in cavities. The blocks (with their triplets of the Ag atoms around the $\text{S}-\text{Au}-\text{S}$ groups) possess a 3-fold symmetry axis or its distorted relics, similar blocks being mutually oriented along four diagonal directions of the cubic or pseudocubic cell in all Ag_3AuS_2 , Ag_3AuSe_2 , and Ag_3AuTe_2 chalcogenides. Note, that the rhombohedral Ag_3AuS_2 contains blocks of two types, with the 3-fold and the pseudo-3-fold axis.

Silver-gold selenide fischerite, Ag_3AuSe_2 ,¹² and telluride petzite, Ag_3AuTe_2 ,¹³ which are isoformular to the sulfide under consideration, are crystallized in cubic unit cells ($a = 9.965$ and 10.385 Å, respectively, in space group $I4_132$). There is no sulfide with the Ag_3AuS_2 composition with a decreased linear metrics of

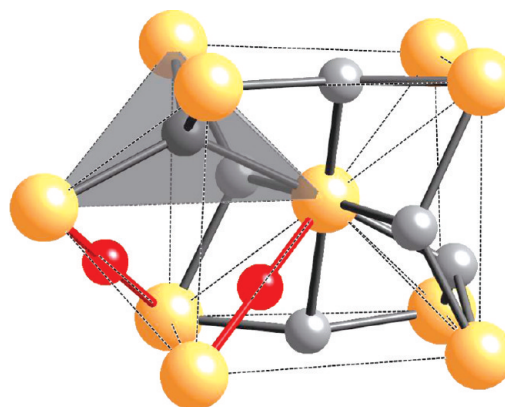


Figure 4. Fragment of the anion packing. At the left, the S_6 octahedron is divided into four tetrahedra (sphenoids); one is occupied by the Ag atom. The Au atoms are situated at the edges of vacant sphenoids.

the unit cell ($a \approx 9.68-9.85$ Å⁷) possessing such a high degree of symmetry. The obvious reason is the difference in linear group lengths causing a distortion of the Ag_3 configuration. Thus, the lengths of the $\text{Se}-\text{Au}-\text{Se}$ and $\text{Te}-\text{Au}-\text{Te}$ groups are 5.20 and 5.22 Å, respectively, but the $\text{S}-\text{Au}-\text{S}$ group is significantly shorter (≈ 4.67 Å). It is important that in jalpaite, Ag_3CuS_2 ,¹⁴ a Cu analogue of Au chalcogenides, the $\text{S}-\text{Cu}-\text{S}$ length decreases to 4.35 Å and the structure is found to be built in a different way.

A close grouping of six Ag atoms around one S atom determines the short $\text{Ag}\cdots\text{Ag}$ distances; as a consequence, the AgS_4 tetrahedra share three or four common edges, which are remarkably shorter than the unshared edges. As a result, the tetrahedra acquire a specific configuration typical of the so-called sphenoids of the body-centered cubic packing.^{15,16} Thus, in our opinion, this configuration of the Ag_6S group is one the factors responsible for this distribution of the sulfur atoms.

In fact, the net of the sulfur atoms is a somewhat distorted body-centered cubic packing (Figure 4). It may be subdivided into vacant octahedra slightly flattened along one of the 4-fold axes. In their turn, each of them is formed of four irregular tetrahedra, or sphenoids, with the shared edge along the decreased diagonal.¹⁶ In the structures of Ag_3AuX_2 chalcogenides, one of four sphenoids is populated by Ag atoms, while three alternative sphenoids remain vacant. The Au atoms are located on short edges of the vacant sphenoids (Figure 4). Note that six similar sphenoids different in orientation fall at each X node of the packing.

The structures of Ag_3AuX_2 chalcogenides may be depicted as infinite tubes arranged along the 3-fold axis (Figure 2) and combined by the shared edges of the Ag tetrahedra. The tubes are multiplied by basic translations of the cubic or pseudocubic unit cell. A building unit of the tube with the $\text{Ag}_{12}\text{Au}_4\text{X}_{20}$ composition includes four linear $\text{X}-\text{Au}-\text{X}$ groups, one of which lies on the 3-fold axis, and two six-member sets of the Ag tetrahedra are around the axial X atoms (Figure 5a). Building units are joined into tubes through six-member sets of common anions, and the tube composition corresponds to $\text{Ag}_{12}\text{Au}_4\text{X}_{14}$. Tubes can be built in different ways.

Building units in a tube in the trigonal structure of the silver-gold sulfide Ag_3AuS_2 are joined by common vertices of the tetrahedra (Figure 5b). In the cubic selenide, Ag_3AuSe_2 , and telluride, Ag_3AuTe_2 , they are joined through common edges (Figure 5c). The difference is in the manner of multiplication of

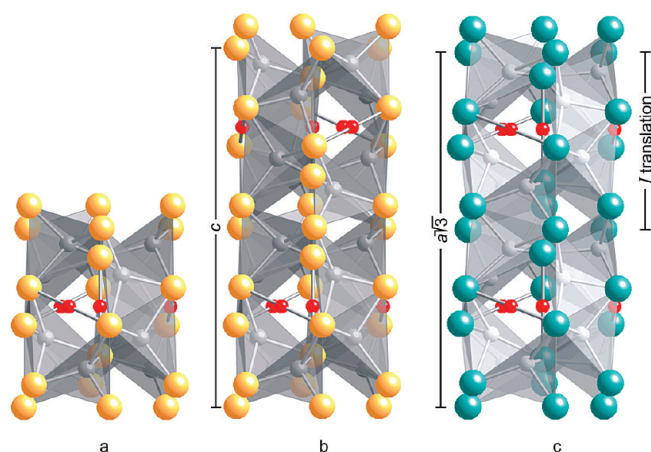


Figure 5. $\text{Ag}_{12}\text{Au}_4\text{X}_{20}$ building unit of the tubes (a) and joining of the blocks along the 3-fold axis in the structure of the studied $\text{Ag}_{2.94}\text{Au}_{1.06}\text{S}_2$ (b) and fischesserite, Ag_3AuSe_2 (c).

building units in tubes. In the petzite-like structure with a (pseudo)cubic body-centered unit cell, they are multiplied by translation along the body diagonal. In the trigonal case, multiplication is realized by means of reflection and a translation shift by the c plane (Figure 5b,c).

Different tubes are joined differently. As a result, in the pseudocubic rhombohedral unit cell, unlike the cubic one, there are tubes only along one body diagonal with a 3-fold axis. The cations of Au and Ag are distributed differently in structures with different symmetries with the same body-centered matrix. Thus, all the AgX_4 tetrahedra are equivalent in the structures of the petzite type, and in particular, they have three common edges. There are two kinds of tetrahedra in the structure of the studied sulfide, and one of them has four common edges. That is why the phase Ag_3AuS_2 cannot be attributed to the petzite group: it is a new structure type.

POLYMORPHISM OF Ag_3AuS_2

The following preliminary conclusion can be made about the polymorphism of Ag_3AuS_2 considering our results and critical analysis of the literature data. It is clear that the cubic phase with the petzite-like structure has not been established. The data of Messien et al.¹ are not satisfactory judging both by the results of the structure refinement ($R = 22\%$) and by its crystallographic characteristics.

Nekrasov⁷ reports the existence of a continuous series of solid solutions, the end members of which are uytenbogaardtite (tetragonal Ag_3AuS_2) and fischesserite (cubic Ag_3AuSe_2). This may be the case if the uytenbogaardtite structure closely resembles that of the petzite one. However, so far, the structure of the tetragonal modification has not been established.

All known samples of the mineral uytenbogaardtite are described in a tetragonal metrics. We have compared calculated diffraction profiles for the cubic structure¹ and model tetragonal petzite-like structure using the experimental powder data.³ The results have shown that the tetragonal phase is not petzite-like.

Unlike the reported modifications, the samples studied in our laboratory as a result of high-temperature synthesis are related to radically different modifications, established first. The data available in the literature testify that in natural and synthetic compounds with the idealized Ag_3AuS_2 formula, the Ag:Au ratio varies within noticeable limits.^{3,7,17} The influence of formation

conditions and stoichiometric deviations on the structure type has already been proven by the available experimental data. However, this question can be answered in detail only after obtaining the lacking structural data.

The mineral liujinyinite^{4,5} with the described idealized formula Ag_3AuS_2 and the metrics of the tetragonal unit cell $a = 10.01 \text{ \AA}$ and $c = 11.11 \text{ \AA}$ ($Z = 8$) sharply falls out of the series under consideration by density. The data should be redetermined.

It should be noted that all the above considered low-temperature modifications are likely to be characterized by the same coordination formula, $\text{Ag}_3^{[4]}\text{Au}^{[2]}\text{S}_2^{(7)}$, unlike the high-temperature phase Ag_3AuS_2 ,¹⁸ where Ag is present as in 4-fold so in 3-fold coordination of S. It means that structural differences of polymorphs and moderate differences in density values are due to differences in the configuration of the cation subsystem.

AUTHOR INFORMATION

Corresponding Author

*E-mail: k.a.kokh@gmail.com.

ACKNOWLEDGMENT

This work was supported by RFFR Grant 08-05-00233a. We thank the staff of the Analytical Center (IGM SB RAS) N. Karmanov, A. Titov, and E. Nigmatulina for their work.

REFERENCES

- Messien, P.; Baiwir, M.; Tavernier, B. *Bull. Soc. R. Sci. Liege* **1966**, *35*, 727–733.
- Graf, R. B. *Am. Mineral.* **1968**, *53*, 496–500.
- Barton, M. D.; Kieft, C.; Burke, E. A. J.; Oen, I. S. *Can. Mineral.* **1978**, *16*, 651–657.
- Chen, Z.; Guo, Y.; Zen, J.; Xu, W. *Kexue Tongbao* **1979**, *24*, 843–848.
- Wei, M. *Dizhi Kexue* **1981**, 232–234.
- Nekrasov, I. Ya.; Lunin, S. E.; Egorova, N. V. *Dokl. Akad. Nauk SSSR* **1990**, *311*, 943–946.
- Nekrasov, I. Y. *Geochemistry, mineralogy, and genesis of gold deposits*; Nauka: Moscow, 1991; p 301.
- Pal'yanova, G. A.; Savva, N. E. *Russ. Geol. Geophys.* **2009**, *50*, 579–594.
- Savva, N. E. In *Mineralogy and Genesis of Gold and Silver Deposits*; SVKNII DVO RAN: Magadan, Russia, 1996; pp 66–81.
- Sheldrick, G. M. *SHELXS-97: A program for automatic solution of crystal structures*, release 97-2; University of Göttingen: Göttingen, Germany, 1997.
- Sheldrick, G. M. *SHELXL-97: A program for crystal structure refinement*, release 97-2; University of Göttingen: Göttingen, Germany.
- Bindi, L.; Cipriani, C. *Can. Mineral.* **2004**, *42*, 1733–1737.
- Chamid, S.; Pobedimskaya, E. A.; Spiridonov, E. M.; Belov, N. V. *Kristallografiya* **1978**, *23*, 483–486.
- Baker, C. L.; Lincoln, F. J.; Johnson, W. S. *Aust. J. Chem.* **1992**, *45*, 1441–1449.
- Bakakin, V. V.; Belov, N. V. *Dokl. Akad. Nauk SSSR* **1979**, *248*, 1329–1331.
- Bakakin, V. V. In *Problems of crystal chemistry*; Porai-Koshits, M. A., Eds.; Nauka: Moscow, 1985; pp 7–38.
- Tavernier, V. B. H. *Z. Anorg. Allg. Chem.* **1966**, *343*, 323–328.
- Folmer, J. C. W.; Hofman, P.; Wiegers, G. A. *J. Less-Common Met.* **1976**, *48*, 251–268.